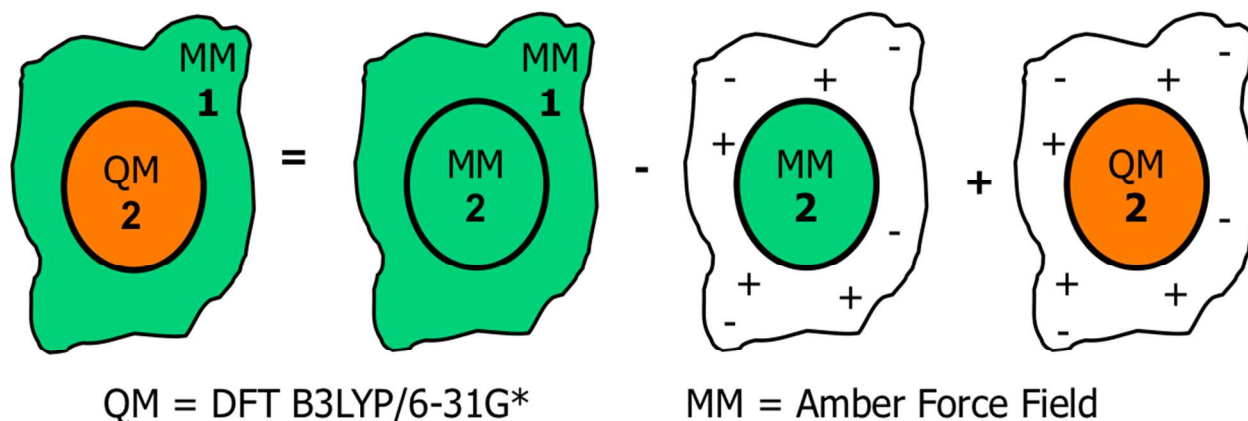# Supporting Information

for

Kinetics of Thermal Activation of an Ultraviolet Cone Pigment

Victoria Mooney[‡], Sivakumar Sekharan[‡], Jian Liu[¶], Ying Guo, Victor S. Batista*, Elsa C. Y. Yan*

QM/MM Scheme:

QM = DFT B3LYP/6-31G*   MM = Amber Force Field

Fig. S1: Schematic representation of the two-layer ONIOM (QM:MM) scheme adopted in this study, where the ONIOM energy is $E^{ONIOM} = E^{MM}_{1+2} - E^{MM}_2 + E^{QM}_2$.

QM/MM calculations were performed with the use of our own n-layered integrated molecular orbital and molecular mechanics (ONIOM) method. In this case, we have used the two-layer ONIOM (QM:MM) scheme (*1-3*), in which the interface between QM (the USB form of 11-*cis* retinyl chromophore) and MM (opsin) region is treated by hydrogen link atom (*4*). To be specific, the total energy of the system (E^{ONIOM}) is obtained from three independent calculations:

$$E^{ONIOM} = E^{MM}_{1+2} - E^{MM}_2 + E^{QM}_2,$$

where E^{MM}_{1+2} is the MM energy of the entire system (including both retinyl chromophore and opsin), called real system in ONIOM terminology; E^{MM}_2 is the MM energy of a part of real system that has main chemical interest (retinyl chromophore, USB in the SHUV pigment and PSB in rhodopsin), called model part (Fig. S1) and E^{QM}_2 is the QM energy of the retinyl chromophore.

In this study, electrostatic interactions between the two layers were calculated using the electronic embedding (EE) scheme. In the EE scheme, the electrostatic interactions between the two layers are present in all the three energy terms. Thus, the electrostatic interaction terms included at the MM energies (E^{MM}_{1+2} and E^{MM}_2) cancel out, leaving only the interaction energy term that also includes polarization of the wave function of the model part (retinyl chromophore) by the surrounding point charges of the opsin (E^{QM}_2). Therefore, according to this QM/MM methodology, the energy of the protein **1**, described at the molecular mechanics (MM) level, with an embedded chromophore **2** described according to quantum mechanical (QM) density functional theory is obtained as the MM energy of the complete system E^{MM}_{1+2} *minus* the MM energy of chromophore E^{MM}_2 interacting with the environment. This DFT-QM/MM protocol has been shown to yield results in excellent agreement with experimental measurements in our previous studies on related retinal proteins (5-16).

Relaxed intermediate structures, along the resulting isomerization minimum energy path, are obtained subject to constraint of incremental changes of the dihedral angle ($\phi_{C11=C12}$) in the *cis* (-18° in SHUV, -17° in rhodopsin) to -180° (*trans*) range, relaxing the configuration of residues within a 4.0 Å radius (Fig.4 B and C in the main text) from any atom of the retinyl chromophore and two waters (Fig. S2) in rhodopsin and SHUV pigment models. The transition state for C11=C12 dihedral angle ($\phi_{C11=C12}$) during the cis-trans isomerization was identified at -96° for SHUV and at -116° for rhodopsin models (17). We calculate that the *cis-trans* isomerization barrier to be significantly lower in the SHUV pigment (~23 kcal/mol) compared to rhodopsin (~40 kcal/mol) (see Table S1). The calculated QM/MM values are in excellent agreement with the calculated values of ~23 and ~45 kcal/mol obtained by Barlow *et al.* (18) using the MNDO/AM1 and INDO/PSDCI molecular orbital theory methods. We attribute the decrease in the isomerization barrier to change in the protonation state of the Schiff base and to the lessening of the steric constraints in the SHUV binding pocket.

Table S1: QM/MM energy decomposition of the reactant and transition state configurations during the *cis-trans* thermal isomerization event in SHUV and rhodopsin pigments.

SHUV (USB)	E^{MM}_2	E^{MM}_{1+2}	E^{QM}_2
Reactant (-18°)	0.023312 (26.743)	-15.973055 (30.066)	-833.928969 (23.171)
Transition (-96°)	0.065930 (0.000)	-15.928597 (0.000)	-833.892044 (0.000)
Barrier: (27.898 − 26.743) + **23.171** = 24.326 kcal/mol			

Rhodopsin (PSB)	E^{MM}_2	E^{MM}_{1+2}	E^{QM}_2
Reactant (-17°)	-0.030196 (34.960)	-16.022583 (32.347)	-834.845031 (40.546)
Transition (-116°)	0.025516 (0.000)	-15.971035 (0.000)	-834.780417 (0.000)
Barrier: (32.347 − 34.960) + **40.546** = 37.933 kcal/mol			
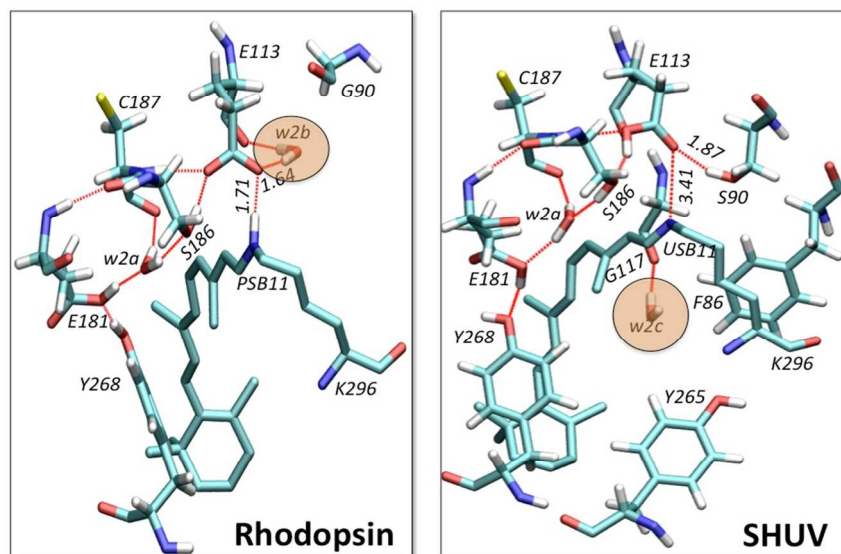
Fig. S2: Comparison of the hydrogen bonding networks in the active sites of bovine rhodopsin and SHUV revealed slight changes in the contributing amino acids (SHUV's S90 → G in rhodopsin), arrangement of the water molecules, change in the orientation of the hydrogen bonds and the evolutionary displacement w2b in rhodopsin to w2c position in the SHUV model.
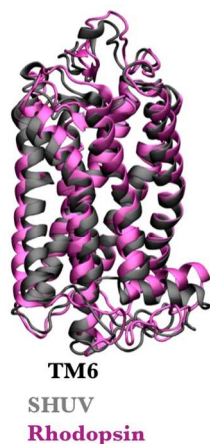
Fig. S3: An overlay of the QM/MM optimized rhodopsin (purple) and SHUV (grey) models. The models are oriented such that TM6 is in front and the extracellular loops are above.

The overlay of the bovine rhodopsin crystal structure and SHUV model is shown below (Figure S3). Focusing primarily on the transmembrane helices and extracellular loop 2, the average displacement of amino acids of the QM/MM SHUV model when aligned with the QM/MM bovine rhodopsin model were revealed by the RMSD values of the alignment of C-alpha atoms. These values (Table S2) reveal that the order of maximum displacement is: H2>H6>H4>H7>H1>H3>H5>EL2. This supports the hypothesis that the placement of transmembrane helix 6 contributes to the greater instability of the SHUV pigment.

Table S2. The average displacement of the amino acids in the transmembrane helices and EL2.

	RMSD (Å)
Helix 1	0.675
Helix 2	2.619
Helix 3	0.548
Helix 4	1.217
Helix 5	0.487
Helix 6	1.306
Helix 7	0.983
EL2	0.425

References:

(1) Warshel, A.; Levitt, M. *J. Mol. Biol.* **1976**, *103*, 227.
(2) Vreven,T.; Morokuma, K.; Farkas, O.; Schlegel, H. B.; Frisch, M. J. *J. Comput. Chem.* **2003**, *24*, 760.
(3) Frisch, M. J.; et al. *Gaussian 09,* Revision A.02; Gaussian, Inc.: Wallingford, CT, 2009.
(4) Bakowies, D.; Thiel, W. *J. Phys. Chem.* **1996**, *100*, 10580.
(5) Gascón, J. A.; Batista, V. S. *Biophys. J.* **2004**, *87*, 2931.
(6) Gascón, J. A.; Sproviero, E. M.; Batista, V. S. *J. Chem. Theory Comput.* **2005**, *1*, 674.
(7) Gascón, J. A.; Sproviero, E. M.; Batista, V. S. *Acc. Chem. Res.* **2006**, *39*, 184.
(8) Sekharan, S.; Altun. A.; Morokuma, K. *Chem. Eur. J.* **2010**, *16*, 1744.
(9) Sekharan, S.; Altun. A.; Morokuma, K. *J. Am. Chem. Soc.* **2010**, *132*, 15856.
(10) Sekharan, S.; Morokuma, K. *J. Am. Chem. Soc.* **2011**, *133*, 4734.
(11) Sekharan, S.; Morokuma, K. *J. Am. Chem. Soc.* **2011**, *133*, 19052.
(12) Sekharan, S.; Yokoyama, S.; Morokuma, K. *J. Phys. Chem. B.* **2011**, *115*, 15380.
(13) Sekharan, S.; Katayama, K.; Kandori, H.; Morokuma, K. *J. Am. Chem. Soc.* **2012**, *134*, 10706.
(14) Sekharan, S.; Wei, J. N; Batista, V. S. *J. Am. Chem. Soc.* **2012**, *134*, 19536.
(15) Pal, R.; Sekharan, S.; Batista, V. S. *J. Am. Chem. Soc.* **2013**, *135*, 9624.
(16) Sekharan, S.; Mooney, V. L.; Rivalta, I.; Kazmi, M. A.; Neitz, M.; Neitz, J.; Sakmar, T. P.; Yan, E. C.; Batista, V. S. *J. Am. Chem. Soc.* **2013**, *135*, 9624.
(17) Guo, Y.; Sekharan, S.; Liu, J.; Batista, V. S.; Tully, J. C.; Yan, E. C. Y. *Proc. Natl. Acad. Sci. U.S.A.* **2014**, *111*, 10438.
(18) Barlow, R. B.; Birge, R. R.; Kaplan, E.; Tallent, J. R. *Nature* **1993**, *366*, 64.